Structural Health Monitoring of a helicopter tail boom using Lamb waves – Advanced data analysis of results obtained with integrated optical fibre sensing technology

Maria Ercsey-Ravasz [1], Fran Fransens [2,3], Helge Pfeiffer [2,4*], Gaël Monavon [5], Caroline Korosec [5], Wolfgang Hillger [6], Sabine Van Huffel [7], Martine Wevers [2]

[1] Peter Pazmany Catholic University, Faculty of Information Technology , Práter utca 50/a, HU-1083, Budapest, Hungary
[2] Katholieke Universiteit Leuven – Group: Materials performance and Non-destructive Evaluation, Kasteelpark 44, 3001 Leuven, Belgium
[3]Groep T (Associatie K.U.Leuven), Vesaliusstraat 13, 3000 Leuven, Belgium
[4] METALogic, Technologielaan 11, 3001, Leuven, Belgium
[5] Eurocopter, Aeroport International Marseille-Provence, 13725 Marignane, France
[6] DLR German Aerospace Center, Institute of Composite Structures and Adaptive Systems, Lilienthalplatz 7, 38108 Braunschweig, Germany
[1] Katholieke Universiteit Leuven – Group: Division SCD-SISTA, Kasteelpark 10, 3001 Leuven, Belgum,
* Corresponding author. Tel.: +32-16-32 12 32; fax: +32-16-32 19 90.
E-mail address: helge.pfeiffer@mtm.kuleuven.be (H. Pfeiffer).

Abstract
Structural health monitoring of an aircraft can enhance operational safety by ensuring that vital structural components are not degraded by impact damage. This study is part of the 6th STREP framework AISHA project, investigating the use of ultrasonic Lamb wave technology for the fast inspection of a helicopter structure. Single mode (SM) optical fibres embedded in a SMARTape and glued on a structural part or embedded in the composite have been used. Quantitative correlations between the monitored transient signals of the optical fibre and the type and extent of the damage are established.

Keywords: Structural Health Monitoring, Optical Fibre Sensor, Sandwich composite, Lamb waves, aerospace

1. Introduction

Lamb waves are promising candidates for the permanent investigation of the structural health of aircraft (structural health monitoring - SHM). SHM can be applied in different ways. In some cases, it is sufficient to perform the measurements offline, i.e. when the aircraft is on the ground. In some cases however, real online monitoring is necessary. This is e.g. the case when impact damage is expected to have immediate influence on vital functions of the aircraft. This holds e.g. for the impact damage in helicopter components made of composite structures. Due to the noisy background, potential impact damage will not be noticed by the crew, especially when such incidents just lead to barely visible impact damage (BVID) while severe core damage has occurred. The detection of such defects by optical fibre technology is well understood and was already successfully applied on samples on lab-scale [1]. In this study, different composite materials (monolithic, sandwich) and impact energies (ranging from 1 to 20 J) were used to derive relationships between signal parameters and the degree of damage. The implementation of that technology into real aircraft structures is however more difficult to achieve. This holds especially for the analysis of the data obtained. In real aircraft structures, a number of multiple reflections of ultrasonic signals occurring at natural reflectors (structural elements, service holes) hiding the information coming from harmful defects. This is the reason why advanced data analysis has to be in place [2]. In this paper, early experiments on impact damage detection in a helicopter tail boom are

presented, and data analysis inspired by image processing is performed. For the detection of the ultrasonic waves, optical fibre technology was used. In contrast to point transducers, optical fibre sensors can monitor large areas without the need to cover the structure with an enormous amount of sensors [3]

2. Experiments

Full scale impact tests were performed on a semi-shell of a composite helicopter tail boom (EC-135 manufactured by Eurocopter, Marignane, France, (Fig. 1)). The detection technique applied is based on the concept presented in [1]. Using this set-up, Lampb waves actuated by a piezoelectric transducer are recorded using an optical fibre sensor working in the polarisation mode [4]. Two SMARTape optical fibre sensors have been attached to the tail boom (about 2,5 m). In the present case, an array of piezoelectric (PZT) sensors is used on each side of the tail boom enabling an approximate localisation of the defect. The information on the position of the corresponding PZT and the signal recorded by the fibre should give approximate information on the position of the defect.

Fig. 1 Part of the helicopter EC135 tail boom.

Impact damages were created on the helicopter tail. This was done by a drop weight with a 16 mm head (Fig. 1) according to the Eurocopter impact test recommendations. By adjusting the drop height, the impact energy could be controlled.

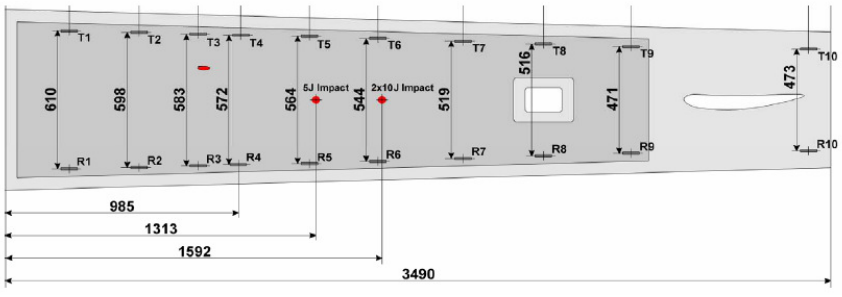

Fig. 2 Positions of transducers at the tail boom

Fig. 2 shows the location of the impacts (two times 5 J). It is clear that they are located between sensors R3-R4 and T3-T4. During impact testing, acoustic emission measurements were additionally performed. Both the PZT sensors and the optical fibre sensor were applied as sensing elements. This means that not intrinsic commercially acoustic emission sensors were used, but the patches originally intended to perform the

active ultrasonic Lamb wave tests. To detect the signals coming from the PZT sensors a 14 channel VALLEN read-out unit (Fig. 3) was used.

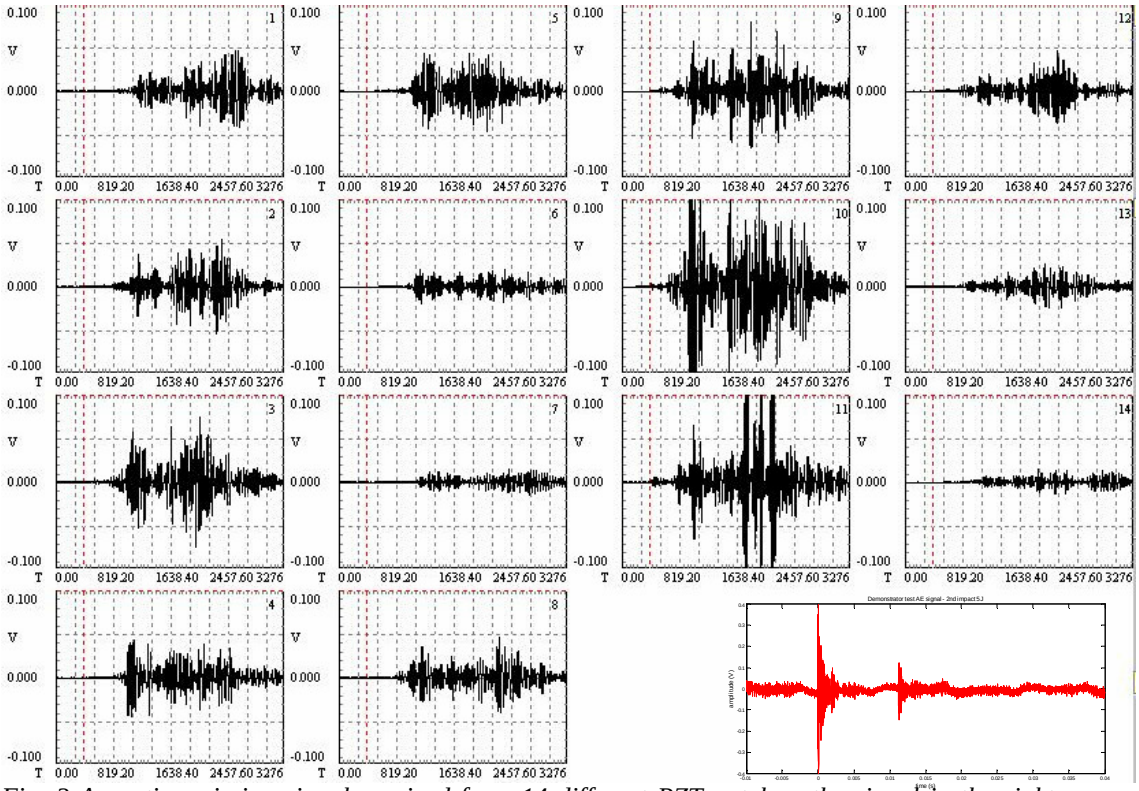

Fig. 3 Acoustic emission signal received from 14 different PZT patches, the signal in the right corner represents the signal received by optical fibre sensor.

The plots in Fig. 3 above shows some examples of the received acoustic emission signals. Such as expected, the amplitude and time of arrival depends strongly on the position of the sensor relative to the impact location. To prove that acoustic emission measurements can also be done by the optical fibre sensors [5], additional measurements were made. A detailed analysis of this test will be given in a subsequent paper. One of the received signals is also shown in Fig. 3 indicating the main burst and one echo. As a main target of this experiment, active Lamb wave testing was performed.

3. Data analysis

Our goal was to detect and locate impact damages in composite materials (like a helicopter tail) by observing changes in the signals measured with the optical fibre. In this section the methods used are described and results obtained in the case of active Lamb wave measurements with optical fibres on an impacted helicopter tail are presented. The time-frequency images of signals obtained before and after the damage were compared. More different parameters characterizing the difference between the images are calculated. One can show that a global view of this set of parameters can give fair information about the position of the impact. The methods were tested not only with real damages, but also with pseudo defects, which are easier to control, but also have a much smaller influence on the signals.

The time-frequency images represent how the power spectrum of the signal changes in time. They are obtained using the Short Time Fourier Transform (STFT). Considering the signal array in time (obtained with the optical fibre), in each step a window with size *W* is used for calculating the power spectrum. Here a rectangular window is used, meaning all data in the window are counted with the same power. In the next step the window is shifted with *I=W/2*. Then the power spectrum of each window is plotted in function of time, this way a *3* dimensional graph, or a coloured image is obtained.

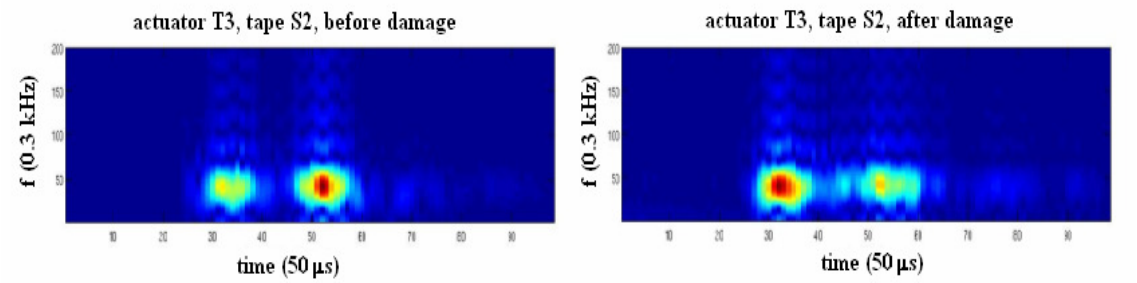

Fig. 4 The time frequency images of the signals obtained using the optical fiber S2, and the actuator T3, before and after the impact was made. The frequency of the signal is 12 kHz, length of the signal array is N=25000, window size W=500, I=250.

Fig. 4 shows the time-frequency image of a signal with 12 kHz measured by the optical fibre S2, when the actuator T3 was used. The first image is constructed from a signal measured before damage was made, and the second one after the impact. The length of the signal arrays was N=25000, W=500 size window is used, and is shifted in each step with I=250. One can see a significant difference between the two images. The reason is that the impact damage is exactly between the T3 actuator and the S2 tape. In case the damage is not so close, the difference becomes much less visible. The question is how these differences can be measured, obtaining useful quantities, without needing to analyse the images with our own eyes.

Different methods are proposed here, first the so called L1 and L2 metric is calculated, frequently used for comparing very similar images. The second method compares the above-level-sets of the images using different levels. With a third method developed one can measure how much some characteristic points changed their positions after the damage was made. As characteristic point one can use the local maximum points on the image, or the points where the gradient is maximal. These three methods are sensible for different kind of changes occurred in the images. If the main frequency peak of the spectrum was shifted because some interferences were caused by the damage, if the amplitude or the shape of the spectrum changed, will all be reflected by the parameters. In the following the methods and the obtained results are described in more details.

3.1 Comparing the images using the L_1 and L_2 metrics

The L_1 and L_2 metrics are two special and most-used [6] cases of the general L_p metric (Minkowski metric). Having two points in an n-dimensional space - in this case the images represented by the pixel-values the L_1 metric is equivalent with the Mean Absolute Error (MAE) and L_2 with the Mean Square Error (MSE). One has to mention here that the time-frequency images calculated are always scaled to the [0,1] interval. This is needed because at different measurements the amplitude and power of signals

can change very much even when no damage was done. Scaling the two images to the same interval, after that comparing them with the L_1 and L_2 metrics one gets information about how much the amplitude of the peaks changed relative to each other.
The results obtained with the two different metrics are usually very similar, fig. 2 shows the L_2 metric measured between the time-frequency images of signals obtained in the experiment with the helicopter tail. The measurements were separately plotted when the R actuators are used with smaller (between 10-13kHz) and higher frequencies (18-23kHz), and when the T actuators were used also with smaller and higher frequencies. On each graph the results for measurements obtained with both optical fibers are presented (S1 tape - red and S2 tape – blue). As described in section 2, the impact damage was made on the helicopter tail at positions being closest to the R3, R4, T3, T4 actuators. Even if there are big fluctuations the results show clearly that the L metrics shows the highest values in the case of actuators 3 and 4, being closest to the damage. As expected the effect of the impact damage can be observed only by using the R actuators and the S1 tape, or the T actuators and S2 tape.

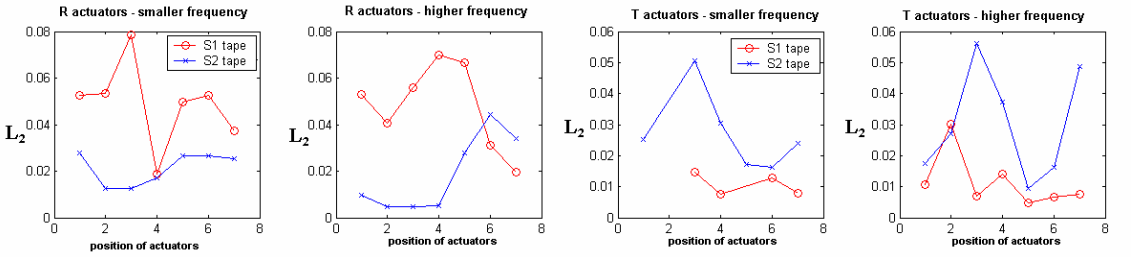

Fig. 5 Results obtained with the L_2 metrics.

3.2 Analyzing the above-level sets of the images

Our second method comparing the time-frequency images of signals obtained before and after damage contains in comparing different above-level-sets of the images. Level sets are widely used for studying shapes that change topology [7,8]. Here we take an image with pixel-values x_i scaled to *[0,1]* and a level c. A threshold operation is performed at the given level, obtaining a binary image in which all pixels will be $y_i=1$ if $x_i>c$, and $y_i=0$, if $x_i<c$. Performing this threshold operation on both images two binary images I_1 and I_2 are obtained. It is interesting how much the place, shape, and area of these sets changed. The parameter is calculated as the following:

$$d(c) = \frac{area(I_1 \ XOR \ I_2)}{area(I_1 \ OR \ I_2)}$$

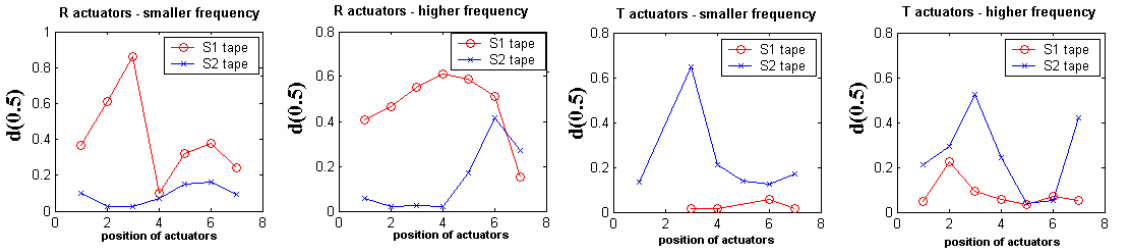

Fig. 6 The parameters calculated for level c=0.5 in function of the position of the actuators.

More exactly the area where the two level-sets do not coincide is divided with the area of the two sets united. This way the parameter d(c) will be 0 if the two sets are exactly the same, and 1 if they are totally different. Fig. 3 shows the results obtained in case of level c=0.5. Similar results are obtained at 0.25 and 0.75. The same observations are true as described at the previous method. Again peaks at actuators 3 or 4 are visible, showing the place of the damage with a good approximation.

3.3 Extracting characteristic points

Our third method is based on measuring how much some characteristic points have changed their position on the image after the damage was made. These characteristic points can be the local maximum points (peaks) of the power spectrum or the points with maximal gradient. The method consists from the following steps:

- First the noisy parts of the image –regions with smaller amplitude than 0.1 – are eliminated.
- The local maximum points are extracted and their positions are saved. Let us name these points X_i, and Y_i, for the first and second image respectively. Usually almost all points on the first image have their correspondent on the second image, of course sometimes new (but usually small) peaks also appear.
- For each point X_i on the first image the closest point on the second image is found, and the distance between them is calculated, let us note these minimal distances: $d(X_i)$. Similarly for the points of the second image one find always the closest point on the first image and again save the distances: $d(Y_i)$.
- These minimal distances are now averaged using a weighted average. The weights w(Xi) are the amplitudes (power) of the spectrum at the given point. To use these weights is important because if a very small peak changes its position (or a new one appears) is not so important, as for the main peak would be. Finally the parameter calculated is the following:

$$p_1 = \frac{\sum w(X_i)\cdot d(X_i)}{\sum w(X_i)} + \frac{\sum w(Y_i)\cdot d(Y_i)}{\sum w(Y_i)}$$

Results for the signals measured on the helicopter tail are presented on Fig.3. Similar behaviour is observed as using the previous methods. The same method can be used extracting the points with maximal gradient (p_2 in Table 1.).

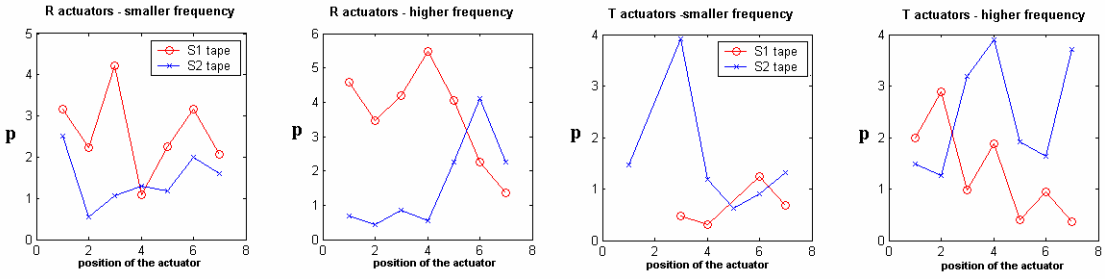

Fig. 7 The parameter, p calculated in case of the local maximum points.

3.4. A global view of the parameters

By measuring all of these parameters one can observe big fluctuations in the curves plotted. This is the reason why it is very important to have a global view about all the

parameters. In Table 1. all the parameters presented characterizing the difference between the time-frequency images of the signals obtained using the T actuators and the S2 optical fiber. In spite of big fluctuation a clear peak can be observed at the T3 and T4 actuators. Similar results were obtained in case of the R actuators using the S1 fibre.

T	L_1	L_2	d(0.25)	d(0.5)	d(0.75)	d(0.9)	P_1	P_2
1	0.008645	0.017515	0.079909	0.212891	0.150238	0.301110	1.489676	2.316136
2	0.011597	0.026978	0.117268	0.294118	0.439274	0.365079	1.262951	3.928570
3	**0.023140**	**0.056225**	**0.375223**	**0.523182**	**0.445084**	**0.367857**	**3.194233**	**5.115065**
4	**0.017370**	**0.037191**	**0.376717**	**0.243051**	**0.207317**	**0.327907**	**3.894683**	**3.651308**
5	0.004707	0.009412	0.074912	0.036677	0.052864	0.075162	1.912661	1.292955
6	0.006533	0.016222	0.131185	0.051764	0.240620	0.279070	1.627867	2.692507
7	0.025464	0.048825	0.420799	0.419246	0.532858	0.912442	3.707742	4.109868

Table 1. Parameter values obtained for the signals measured with the T actuators and S2 optical fibre, on higher frequencies.

Big fluctuations can be seen in the calculated values. In this kind of measurements this is not unexpected of course, and the biggest fluctuations can be seen in case of the actuators 1st and 7th, these being already close to the side of the helicopter tail, or to the gap (insert for the antenna). The difference between two signals measured in exactly the same condition is usually in the range of [0.001-0.005].

3.4. Testing the method with artificial defects

The method was also tested using pseudo defects. These pseudo defects are rubber disks with a diameter of about 4 cm that are attached to the skin of the composite by a couplant (vacuum grease). Pseudo defects disturb the wave propagation of certain Lamb modes similar as in the case real defects, but they have the advantage of easy handling. One can change the position of the "defects" many times, contrary to real impacts, where the damage is irrevocable. On the other hand pseudo defects may cause much smaller changes in the signal measured in the optical fiber, so these are much harder to observe and measure, and fluctuations are expected to be much higher. Moreover, Lamb modes with particle displacements in line with the surface are also quite insensitive to pseudo-defects.
The pseudo defect was placed at different *x* coordinates along 3 rows with y=1,3,5, and 22 kHz frequency was used (the coordinates can be seen on Fig. 5a). The actuator is at coordinates (5,0), and the optical fibre is placed at y=6. It is expected that in each row the maximal disturbance is obtained at x=5, closest to the actuator.

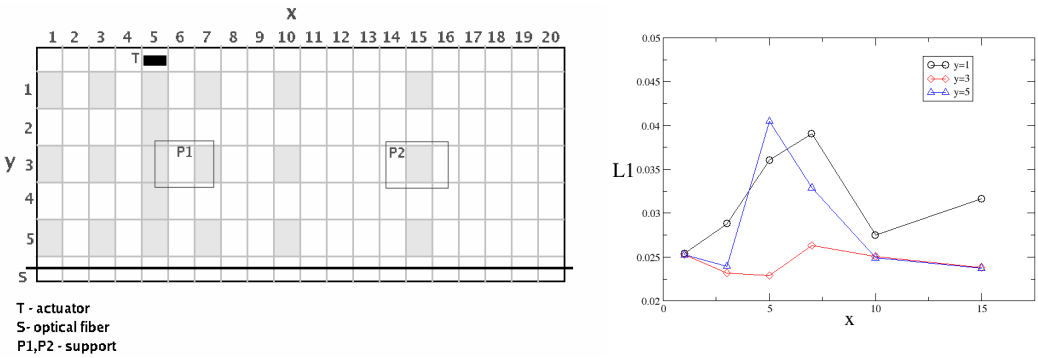

Fig. 8 Pseudodefect positions at the composite plate and parameters obtained.

Results show that for y=1 and y=5 the measurements are as expected, a peak is visible at x=5, where the actuator is (the L1 metric is plotted on fig. 5b., results for the other parameters are also similar). In case of row y=3, the peak is not so clear, this is probably caused by the fact that the two points of support for the plate (P1 and P2) are also at y=3, so at these coordinates the amplitude of the wave and this way the caused perturbation is much smaller.

Acknowledgements

All experiments have been carried out in the frame of the 6th Framework STREP project nr. 502907: Aircraft Integrated Structural Health Assessment (AISHA). We wish to thank all our partners for their support: METALogic, Leuven, Belgium; Deutches Zentrum für Luft- und Raumfahrt (DLR) - German Aerospace Centre, Braunschweig, Germany; Riga Technical University, Riga, Latvia; Eurocopter, Marignane, France; Cedrat Technologies, Meylan, France; Centro de Tecnologías Aeronáuticas (CTA), Miñano (Álava), Spain; ASCO, Zaventem, Belgium
We also wish to thank SMARTEC, Manno, Switzerland for providing the SMARTape fibre sensors.

This research was conducted with the dedicated help from Ing. Johan Vanhulst of K.U.Leuven-Dept. MTM.

References

1. M. Wevers and F. Fransens. Ultrasonic Lamb wave inspection of aircraft components using integrated optical fibre sensing technology, Proceedings of the European Conference of non-destructive testing, September, 25-29, Berlin 2006.
2. W. Staszewski, C. Boller and J.R. Tomlinson, Health Monitoring of Aerospace Structures: Smart Sensor Technologies and Signal Processing, Wiley, Chichester, 2004.
3. G. Thursby, B. Sorazu, D. Betz, W. Staszewski and B. Culshaw. Vol. 5384, pp. 287-295.
4. G. Thursby, B. Sorazu, F. Dong and B. Culshaw. Vol. 5050, pp. 61-70.
5. S. Vandenplas, J.M. Papy, M. Wevers and S. Van Huffel, Acoustic emission monitoring using a multimode optical fibre sensor Insight 46 (2004) 203-209.
6. S. Santani, R. Jain, "Similarity measures", IEEE Trans. on Pattern Analysis and Machine Intelligence, vol. 29, no. 9, pp. 871-883, 1999.
7. S. J. Osher, R. P. Fedkiw, “Level Set Methods and Dynamic Implicit Surfaces”, Springer-Verlag, 2002.
8. S. Osher, N. Paragios, “Geometric Level Set Methods in Imaging, Vision and Graphics”, Springer-Verlag, 2003.